

Zr-2.5Nb

K_{IH}

Behaviors of K_{IH} by Crack Directions and Supersaturated Concentration of Hydrogen in Zr-2.5Nb Pressure Tube

*, , , ,

150

Zr-2.5Nb DHC , DHC
 60 ppm Zr-2.5Nb , CCT
 CB . DHC 160 ~ 280 °C (K_{IH})
 . 160 ~ 250 °C K_{IH} 5.84 MPa√m 8.4 MPa√m
 K_{IH} 가 , K_{IH} 가 ,
 가 280 K_{IH} 가 ,

Abstract

The aim of this study was to obtain a better understanding of delayed hydride cracking (DHC) of Zr-2.5Nb pressure tube with temperature and crack growth direction. DHC tests were conducted at temperatures ranging from 160 ~ 280 °C on Curved Compact Tension (CCT) and Cantilever Beam (CB) specimens with 60 ppm H to determine the threshold stress intensity factor, K_{IH} in axial and radial directions of the Zr-2.5Nb tube, respectively. Over a temperature range of 160 ~ 250 °C, K_{IH} for the Zr-2.5Nb tube 5.84 MPa√m in the axial direction and 8.4 MPa√m in the radial direction, both of which were constant independent of temperatures, However, at 280 , K_{IH} increased unexpectedly to a higher value. Based on the results, K_{IH} for Zr-2.5Nb tube is discussed with the fracture surface and a supersaturated concentration of hydrogen.

1.

Zr-2.5wt%Nb

가 [1], matrix Delayed
 Hydride Cracking (DHC) (Hydride)
 [2]. , rolled joint
 , 가 DHC 가
 , 1983
 hydride blister
 [3]. 1, 2, 3, 4 CANDU [4],
 DHC 가 .
 DHC Fig. 1 . I (K_I) 가
 DHC 가 가 K_I 가 가 .

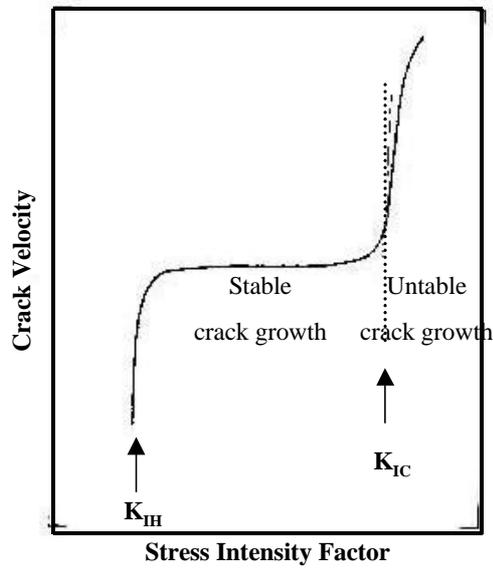


Fig. 1 Effect of stress intensity factor on delayed hydride crack velocity

II K_I 가가 DHC . I K_{IH}
 DHC (critical stress intensity factor) , 가
 , K_{IH} 가
 K_{IH}

2.

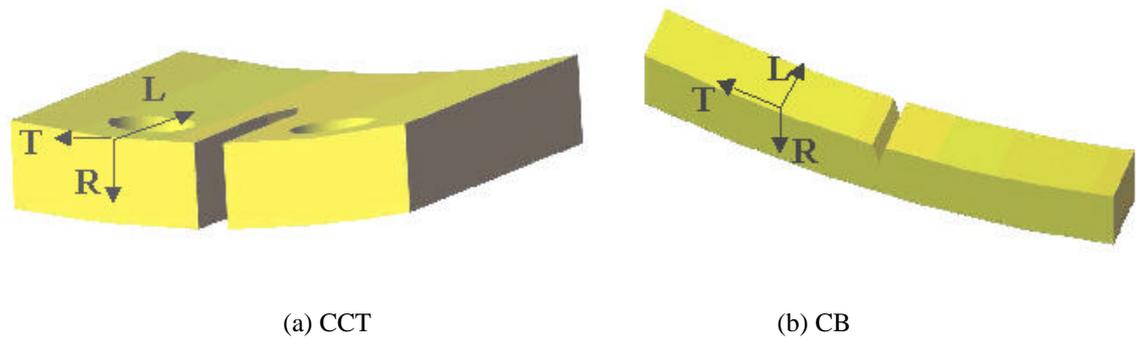
2.1

CANDU 4 cold-worked Zr-2.5Nb .

800°C 11:1 Hot Extrusion Cold Drawing (25%) 400 °C 24 Auto clave
 . CANDU
 800 MPa ($f_t=0.61, f_r=0.33, f_l=0.07$)
 (11:1)

Fig. 2 CANDU

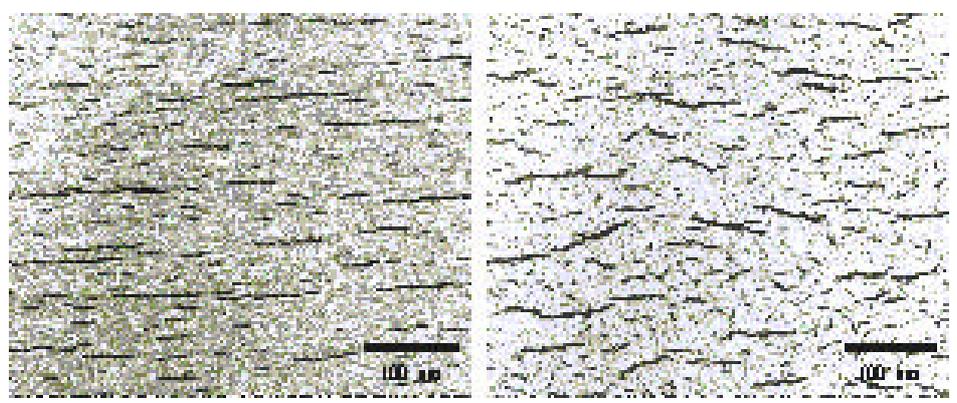
CCT(Curved Compact Tension) CB(Cantilever Beam) . Fig. 2(a) CCT
 20.4mm, 17mm , Fig. 2(b) CB 3.5 mm, 38 mm .



(a) CCT (b) CB
 Fig. 2 Schematic Illustration of Cantilever Beam (CB) and Curved Compact Tension (CCT)

2.2

(Cathodic Hydrogen Charging
 Method) 60 ppm .
 KAERI [5]
 2 () 65±5°C 0.1~0.2 molar ()
 , 150 mA/cm² 23 가 , 50%



(a) Axial Section (b) Circumferential Section

Fig. 3 Morphology Comparison of 60 ppm Hydride after Furnace Cooling

60 ppm

302°C

33

(furnace cooling)

Fig. 3

Hot Vacuum Extraction

2.3

CB (Acoustic Emission) DHC
 K_{IH} CCT DCPD K_{IH}
 DHC Fig. 4

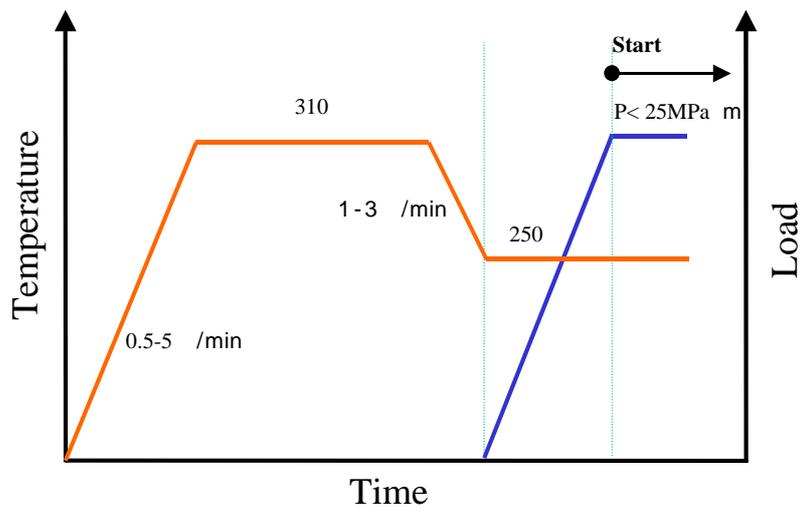


Fig. 4 DHC Condition

K
 ~25 MPa·m
 , soaking
 , soaking
 , DHC soaking 가
 [6]. 가 - controller
 . DHC , Zr-2.5Nb [5] K_{IH}
 , stereoscope SEM

12
 0.5~5°C soaking
 DHC

20 MPa·m
 310 °C 1 1~2 °C/min

3.

3.1

CB CCT K_{IH}
 가 160 ~ 280 °C DHC
 K_{IH}

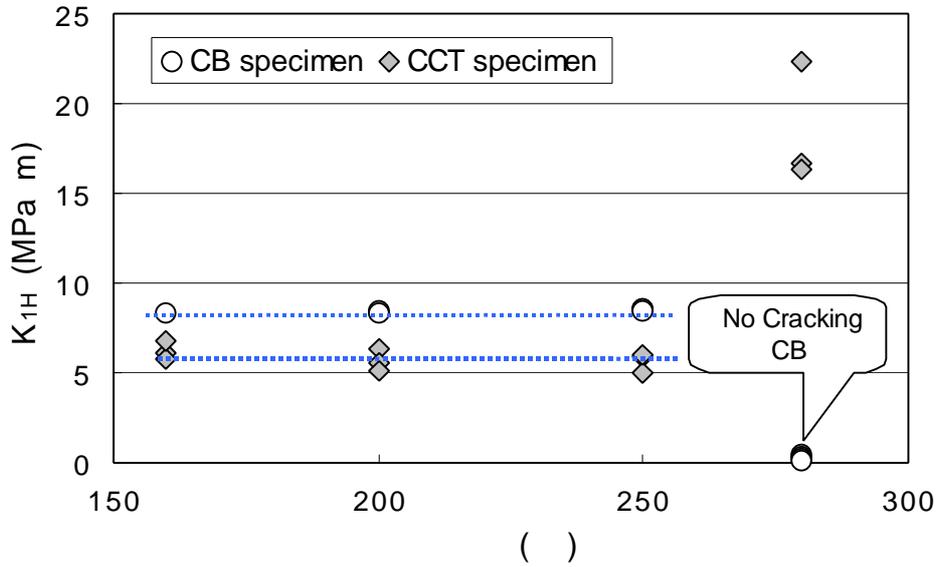


Fig. 5 Comparison of K_{IH} between CB and CCT

Fig. 5 K_{IH} 가 160 ~ 250 °C K_{IH} , 280 °C CCT 16 20 가 , CB

Fig. 6 160 ~ 250 °C K_{IH} 가 가 K_{IH} K_{IH} 5.84 $MPa\sqrt{m}$, 8.44 $MPa\sqrt{m}$ 가

K_{IH} DHC , K_{IH} DHC

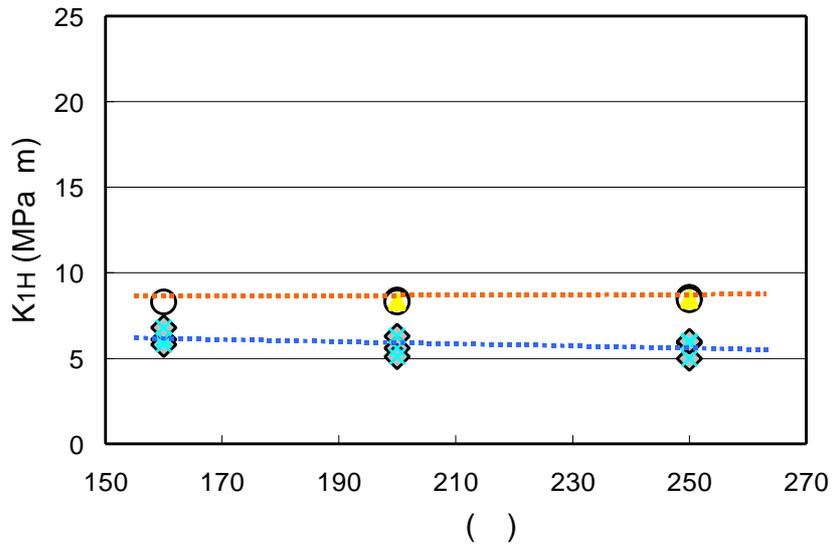


Fig. 6 Comparison of K_{IH} between CB and CCT (160 ~ 250 °C)

K_{IH} , DHCV 1.5, DHCV 2 [7-12].
 가 DHCV 가
 K_{IH} [8, 9].

3.2 K_{IH}
 60 ppm K_{IH} Fig. 5, 6 160 ~ 250, Fig. 5
 280 CCT, 16 ~ 22MPa $\ddot{O}m$, CB, DHC
 K_{IH} 가
 Fig. 7 ?C(-TSSD) K_{IH}
 가 ?C(-TSSD) Puls TSSD[15]
 160 6 ppm, 200 14 ppm, 250 32 ppm, 280 49
 ppm (TSS) 가

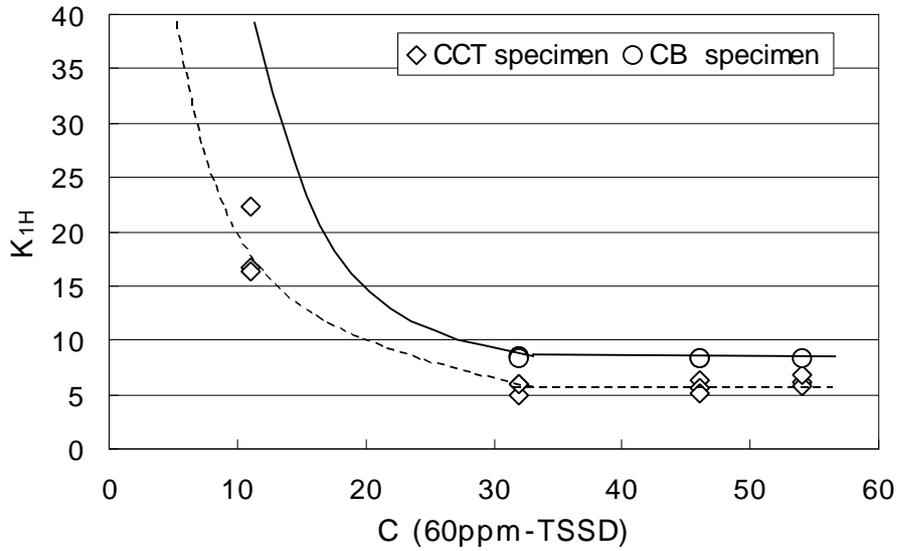


Fig. 7 Hydrogen concentration (? C) dependence of K_{IH} for CB and CCT at 280

60 ppm, Zr
 (terminal solid solubility) 가 160 56 ppm 280
 11 ppm 280 °C DHC 가
 가 matrix, K_{IH}
 K_{IH} (? C), 60 ppm 280 °C
 DHC K_{IH}

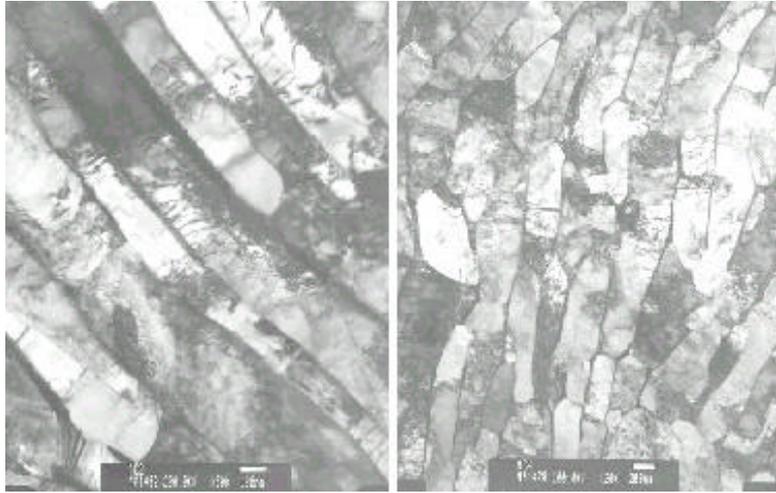
3.3

Fig. 8

(11:1

)

Zr-2.5Nb



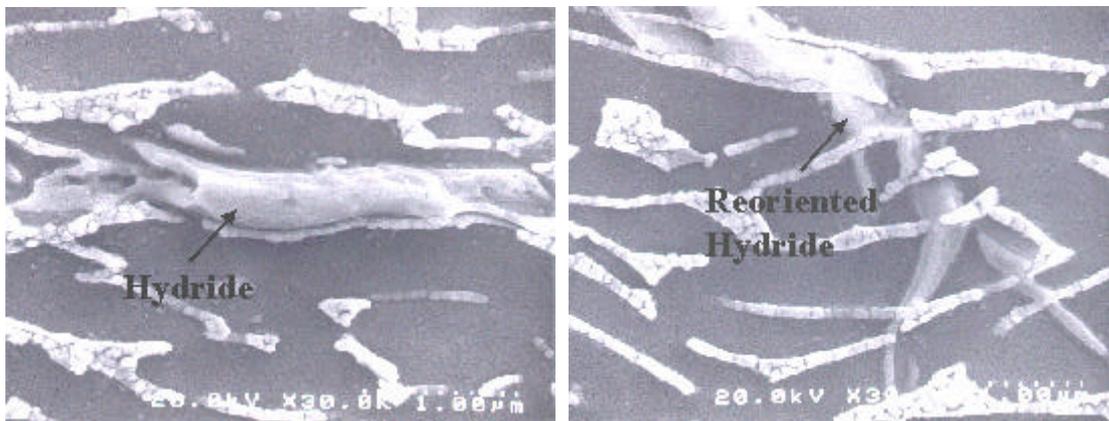
(a) Axial Section

(b) Circumferential Section

Fig. 8 Typical Microstructure of Zr-2.5Nb Pressure Tube

lum -Zr -Zr -Zr
 Fig. 9
 Fig. 9(a) Axial-section a-Zr

Fig. 9(b) DHC 가 Fig. 9(a) DHC a-Zr



(a) Initial hydride before DHC test

(b) Reoriented hydride after DHC test

Fig. 9 Typical Microstructure of Circumferential Hydride and Reoriented Hydride on Zr-2.5Nb Pressure Tube by SEM images

Fig. 10 CB CCT

DHC

Fig. 10(a) CCT

, Fig. 10(b) CB

, DHC

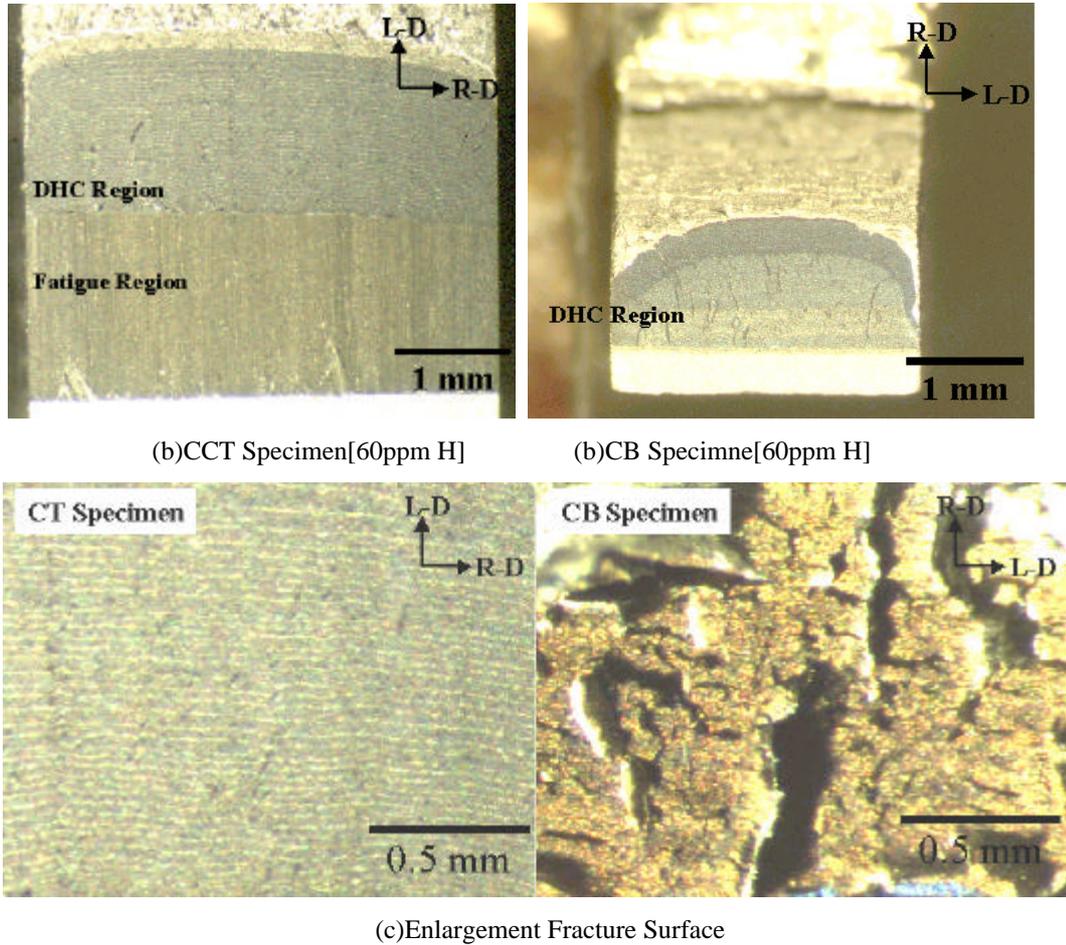


Fig. 10 Fractured Surface of CCT and CB specimen

4.

CANDU Zr-2.5Nb	60 ppm	CCT	CB	DHC	160 ~ 280
°C	K_{IH}				
(1)	K_{IH} 160 ~ 250	가			5.84 $MPa\sqrt{m}$,
(2)	8.44 $MPa\sqrt{m}$				K_{IH} 가
(3)	280	K_{IH}	18.4 $MPa\sqrt{m}$ 가		

- [1] IAEA, IAEA-TECDOC-684, IAEA, Vienna, 1993, pp.7-56.
- [2] B.A. Cheadle et als, ASTM STP 939, ASTM, Philadelphia, 1987, pp.224-240.
- [3] E. G. Price : AECL Report, AECL-8338 (1984)
- [4] KINS, " 1 , 1994
- [5] KAERI, "Zr-2.5Nb , " KAERI/TR-1329/99
- [6] G.K. Shek and D.B. Graham, "Effects of Loading and Thermal Maneuvers on Delayed Hydride Cracking in Zr-2.5Nb Alloys," ASTM STP 1023, 1989, pp. 89-110
- [7] S. Sagat, C. E. Coleman, M. Griffiths, and B. J. S. Wilkins, Zirconium in the Nuclear Industry, Tenth International Symposium, ASTM STP 1245, 1994, pp. 35-61.
- [8] S. S. Kim, S. C. Kwon, and Y. S. Kim, J. Nucl. Mater. Vol. 273, 1999, pp.52-59.
- [9] C. E. Coleman, Zirconium in the Nuclear Industry, Fifth Conference, ASTM STP 754, 1982, pp. 393-411.
- [10] H. Huang, & W. J. Mills, Metal. Transactions A 22A (1991), pp.2149-2060.
- [11] W. J. Mills, and F. H. Huang, Eng. Frac. Mech. 39 (1991), pp. 241-257.
- [12] S. S. Kim, K. N. Choo, S. B. Ahn, S. C. Kwon, Y. S. Kim, and I. L. Kook, Proceedings of the Korean Nuclear Society Spring Meeting, Seoul, Korea, May, 1998, 93-98.
- [13] D. G. Westlake : J. Nucl. Mater., 26 (1968) 208
- [14] Young-Suk Kim : J, kor, Inst. Met. & Mater. Vol.38, No.1(2000)
- [15] Z. L. Pan, M. P. Puls, "The terminal solid solubility of hydrogen and deuterium in Zr-2.5Nb alloys", J. Nucl. Mater., 228, pp. 227-237.